Carbohydrate Polymers 113 (2014) 1–8

Contents lists available at ScienceDirect

Carbohydrate Polymers

journal homepage: www.elsevier.com/locate/carbpol

Cellulose extraction from *Zoysia japonica* pretreated by alumina-doped MgO in AMIMCl

Le Liu, Meiting Ju*, Weizun Li, Yang Jiang

College of Environmental Science and Engineering, Nankai University, Tianjin 300071, PR China

ARTICLE INFO

Article history:
Received 24 March 2014
Received in revised form 28 May 2014
Accepted 19 June 2014
Available online 1 July 2014

Keywords:
Alumina-doped MgO
Extraction
Ionic liquid
Regenerated cellulose

ABSTRACT

In this study, alumina-doped MgO was produced as a solid alkali for lignocellulose pretreatment. Pretreatment with alumina-doped MgO disrupted the lignocellulose structure and significantly reduced the lignin content of the *Z. japonica*. After pretreatment, *Z. japonica* showed significant solubility in 1-allyl-3-methylimidazolium chloride (AMIMCl). The similar high solubility of pretreated *Z. japonica* samples by original alumina-doped MgO and used alumina-doped MgO also proved that alumina-doped MgO had strong stability, which can be recycled and used repeatedly. The regenerated cellulose was similar to microcrystalline cellulose according to FTIR and NMR analyses. Compared to microcrystalline cellulose, only the crystallinity of the regenerated cellulose decreased.

1. Introduction

In China, the "National Long-Term Science and Technology Development Plan (2006–2020)" points out that agricultural biomass is one of the key development areas. Plants, which produce 100 billion tons of cellulose through photosynthesis annually (Zhu et al., 2006), are regarded as an inexhaustible and renewable resource. Plant-derived cellulose is widely used in the textile, chemical, pharmaceutical, and energy industries because it does not contribute to pollution and is biocompatible, biodegradable, and abundant (Zhang, Lv, & Luo, 2011). Moreover, agricultural solid wastes can be used as important lignocellulosic feedstock (Heinze & Liebert, 2001; Zhu et al., 2006). Although the biochemical conversion of biomass into energy and industrial raw materials has significant technical and economic potential, lignocellulosic biomass is naturally resistant to chemical degradation. This resistance is due to various physical and chemical factors, such as the presence of lignin, the crystallinity of cellulose, and the presence of covalent cross-linkages between lignin and hemicelluloses in the plant cell wall (Li et al., 2010). Cellulose is a linear homopolymer of β(1→4)-linked D-glucopyranose units that may aggregate to form a highly ordered structure. The chemical constitution and spatial conformation of cellulose account for its aggregation tendencies (Klemm, Philipp, Heinze, Heinze, & Wagenknecht, 1998; Oh et al., 2005).

Various pretreatment techniques were used to enhance the breakdown of lignocellulosic biomass. However, these technologies commonly use soluble acidic or basic chemicals and result in pollution. Therefore, these chemicals must be recycled, and complex waste-water treatment systems are indispensable in this process. To solve these problems, a novel pretreatment method with a recoverable solid alkali was studied. In the present process of biomass utilization, the removal of lignin is a key step. Cellulose and some hemicellulose are separated from the lignocelluloses through the removal of lignin, and then are hydrolyzed and transformed. But the present methods of lignin removal mainly use chemicals to provide an alkaline condition. These chemicals will result in pollution. Therefore, this study tries to use an insoluble Mg-based solid alkali instead of the soluble alkali to provide a new delignification medium condition. Many types of solid alkalis have been investigated in trans-esterification reactions in the biodiesel or other industries (Sun et al., 2010), including alkali and alkali earth metal oxides (Ebiura, Echizen, Ishikawa, Murai, & Baba, 2005), calcined hydrotalcites (Cantrell, Gillie, Lee, & Wilson, 2005; Xie, Peng, & Chen, 2006), zeolites (Peterson & Scarrah, 1984) and anion exchanged resins (Leclercq, Finiels, & Moreau, 2001). Solid alkali was used for lignocellulosic materials pretreatment in recent years. In 2002, Pang et al. introduced a novel method of cooking corn stalk with solid alkali and active oxygen for pulp production (Pang et al., 2012). Studies also reported that solid alkali was used as a catalyst for lignin degradation and polyurethane synthesis (Sun, 2012; Wang, 2012).

* Corresponding author at: College of Environmental Science and Engineering, Nankai University, 94 Weijin Street, Tianjin 300071, China. Tel.: +86 13672031215.
E-mail addresses: jumeit@nankai.edu.cn, yingying0913@126.com (M. Ju).

http://dx.doi.org/10.1016/j.carbpol.2014.06.067
0144-8617/

Ionic liquids, known as low-temperature molten salts or designable solvents, have been recognized to comprise a new kind of green solvent (Deng, 2003). They offer various advantages that allow them to be widely used in chemical synthesis, extraction and separation, materials preparation, and other fields. Ionic liquids consist solely of cations and anions that are present in liquid form at or near room temperature. Ionic liquids have unique physical and chemical properties, such as low melting point (up to 173 K), higher solubility, and designable selective dissolution (Benoit, Peter, & Moreau, 2004). In 2002, Rogers et al. first reported the solubility of natural cellulose in a series of ionic liquids such as 1-butyl-3-methylimidazolium chloride (BMIMCl) (Swatloski, Spear, Holbrey, & Rogers, 2002). BMIMCl is a nonvolatile, strong solvent for cellulose and is easily recovered after processing. These attributes prompted further research on the regulation and design of cation–anion structures to obtain new types of ionic liquids with superior properties. In 2003, Ren et al. introduced the allyl group to the cationic structure of an ionic liquid to prepare 1-allyl-3-methylimidazolium chloride (AMIMCl), which has excellent solvent properties (Ren, Wu, Zhang, He, & Guo, 2003).

In the present study, alumina-doped MgO is used as a solid alkali, having a weak solubility in water, which can be reused by calcinations after recycling from the cooking effluent. *Zoysia japonica* was pretreated by alumina-doped MgO in a stainless reactor. We focused on the dissolution of pretreated samples in AMIMCl upon ultrasonic treatment. The regenerated cellulose was characterized by Fourier transform infrared (FTIR) spectroscopy and nuclear magnetic resonance (NMR) analyses. This paper provides the necessary theoretical basis for the application of solid alkali for utilization of biomass feedstock resources.

2. Materials and methods

2.1. Materials

Samples of *Z. japonica* were collected from agricultural fields in Tianjin in northern China. After drying at 60 °C in an oven for 16 h, the grass samples were ground to particles that pass through a 0.7 mm screen. The fiber components of *Z. japonica* were analyzed according to the Van Soest method, using a FOSS Fibertec 2010 fully automated fiber analysis system. This determination revealed the following composition: lignin, 19.87% (w/w); hemicellulose, 40.86% (w/w); cellulose, 29.71% (w/w). Microcrystalline cellulose was purchased from Serva (Heidelberg, Germany). AMIMCl was synthesized from *N*-methylimidazole and allyl chloride in our laboratory (Liu, Ju, Li, & Hou, 2013). MgO powder (purity 99.95%) and Al_2O_3 powder (purity 99.997%) were purchased from Tianjin Xuanyang (Tianjin, China).

2.2. Preparation of alumina-doped MgO

MgO powder and Al_2O_3 powder were mixed in de-ionized water and then wet ball-milled to decrease the particle size. MgO powder to Al_2O_3 powder ratio was set at 1:9 (w/w). The mixture was then heated for 5 h at 105 °C to remove the water. The powder obtained as a product was isostatically pressed into a rod and then sintered at 550 °C for 6 h to produce the final sample material.

2.3. Pretreatment of Z. japonica

Z. japonica was loaded into a stainless reactor charged with 200 mL 50/50 (v/v) water-ethanol co-solvents and treated with alumina-doped MgO for 2 h at 160 °C. The solid alkali to *Z. japonica* ratio was set at 1:10 (w/w). Alumina-doped MgO was used 4 times for *Z. japonica* pretreatment. Measurements were recorded for each pretreatment reaction to assess the activity and stability of alumina-doped MgO. When the reactor was cooled to room temperature, the mixture was filtered with Buchner funnel to separate pretreated *Z. japonica* from the filtrate. The pretreated *Z. japonica* was washed with deionized water, then filtered through a nylon membrane and air-dried. *Z. japonica* treated with alumina-doped MgO are denoted as follows: Z_1 (*Z. japonica* treated with original alumina-doped MgO), Z_2 (*Z. japonica* treated with solid alkali used for the second time), Z_3 (*Z. japonica* treated with solid alkali used for the third time), and Z_4 (*Z. japonica* treated with solid alkali used for the fourth time). The lignocellulose residual rate and mass loss rate of *Z. japonica* after pretreatment were calculated according to Eqs. (1) and (2):

$$R_{s,i} = \frac{M_{r,i}}{M_{o,i}} \quad (1)$$

$$R_l = 1 - \frac{M_{rZJ}}{M_{oZJ}} \quad (2)$$

where i represents cellulose, hemicellulose, and lignin; $R_{s,i}$ is the residual rate; $M_{r,i}$ is the mass of the residual cellulose, hemicellulose, or lignin in the *Z. japonica* sample after pretreatment; $M_{o,i}$ is the mass of cellulose, hemicellulose, or lignin in the original *Z. japonica* sample; R_l is the mass loss rate; M_{rZJ} is the mass of the residual *Z. japonica* sample after pretreatment; M_{oZJ} is the mass of the original *Z. japonica* sample.

Organic solvents in the filtrate were removed with an evaporator under reduced pressure at 40 °C and water was further evaporated at 60 °C. The remaining oily product was vacuum dried at room temperature overnight to remove the residual water and defined as degraded *Z. japonica* (DZ, water-ethanol soluble fraction).

2.4. Dissolution of cellulose

The dissolution of *Z. japonica*, pretreated *Z. japonica* and MCC samples in AMIMCl under an argon atmosphere were investigated. For the dissolution process, 2.00 g of sample was added to 50.00 g of ionic liquid (Li, Ju, Wang, Liu, & Jiang, 2013). The mixture was placed in a KQ3200DE ultrasonic oscillator with ultrasonic power 110 W at 80 °C for 30 min (Liu et al., 2013). The remaining insoluble residue was filtered under vacuum using a 60 mL G3 sand-core bush funnel. The resulting filtrate containing the cellulose was collected

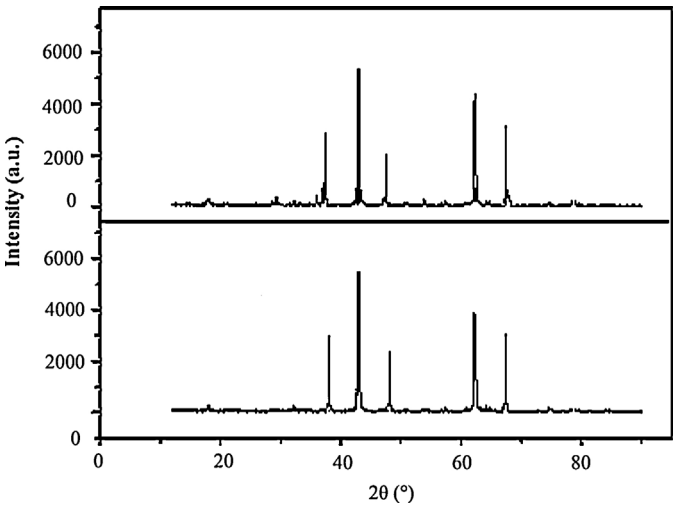

Fig. 1. XRD spectra of alumina-doped MgO (A) and the solid alkali used for the fourth time (B).

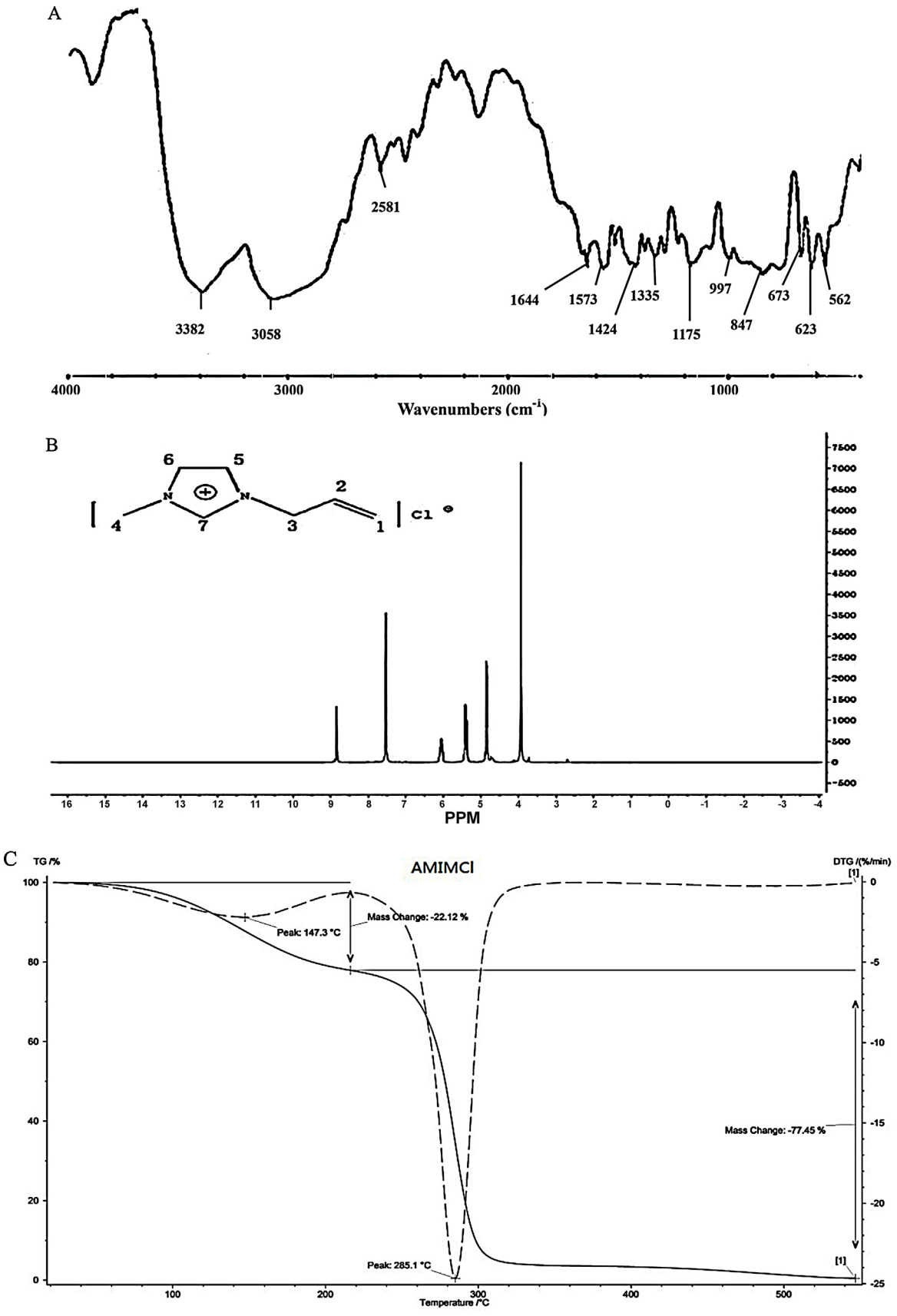

Fig. 2. FTIR spectrum of AMIMCl (A), ^{1}H NMR spectrum of AMIMCl (B) and TGA/DTG curve of AMIMCl (C).

to regenerate the cellulose. The solubility of the sample in AMIMCl was calculated as shown in Eq. (3):

$$R_d = 1 - \frac{M_r}{M_o} \quad (3)$$

where R_d is the solubility in AMIMCl; M_r is the mass of the residual sample after dissolution in AMIMCl; M_o is the mass of the original sample.

2.5. Preparation of the regenerated cellulose

After dissolution of the samples in AMIMCl, the resulting filtrate containing cellulose was combined with an excess amount of deionized water to regenerate the cellulose. The regenerated cellulose samples were dried at 80 °C for 72 h. The cellulose regeneration rate was calculated as shown in Eq. (4):

$$R_r = 1 - \frac{M_{r\text{-}cel}}{M_{o\text{-}cel}} \quad (4)$$

where R_r is the cellulose regeneration rate; $M_{r\text{-}cel}$ is the mass of residual cellulose in the sample after dissolution in AMIMCl; $M_{o\text{-}cel}$ is the mass of cellulose in the original sample.

2.6. Recycling of AMIMCl

After sample dissolution and cellulose extraction, recovery of the AMIMCl was accomplished by evaporating water from the

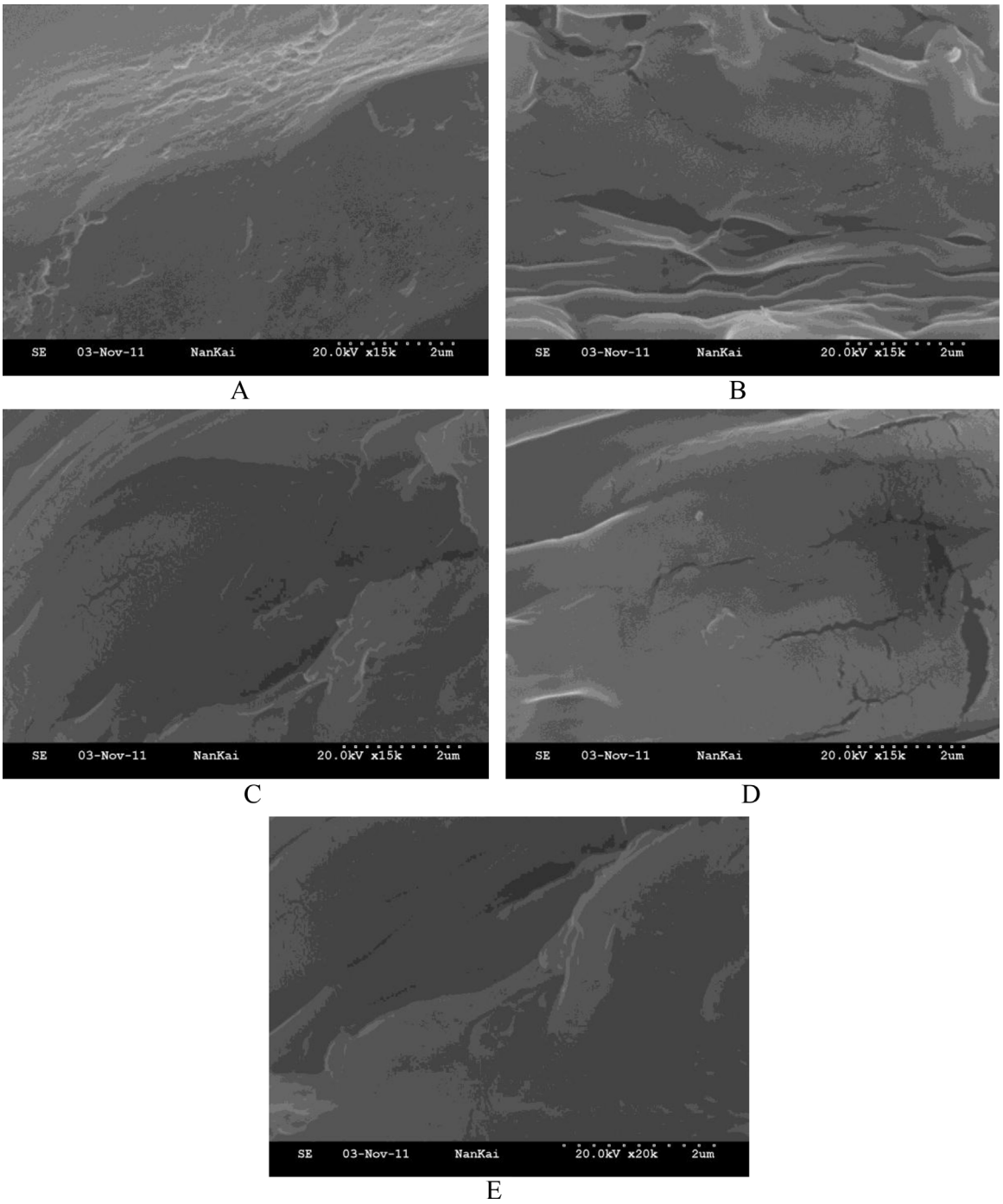

Fig. 3. Structures of original *Zoysia japonica* (A), Z_1 sample (B), Z_2 sample (C), Z_3 sample (D) Z_4 sample (E).

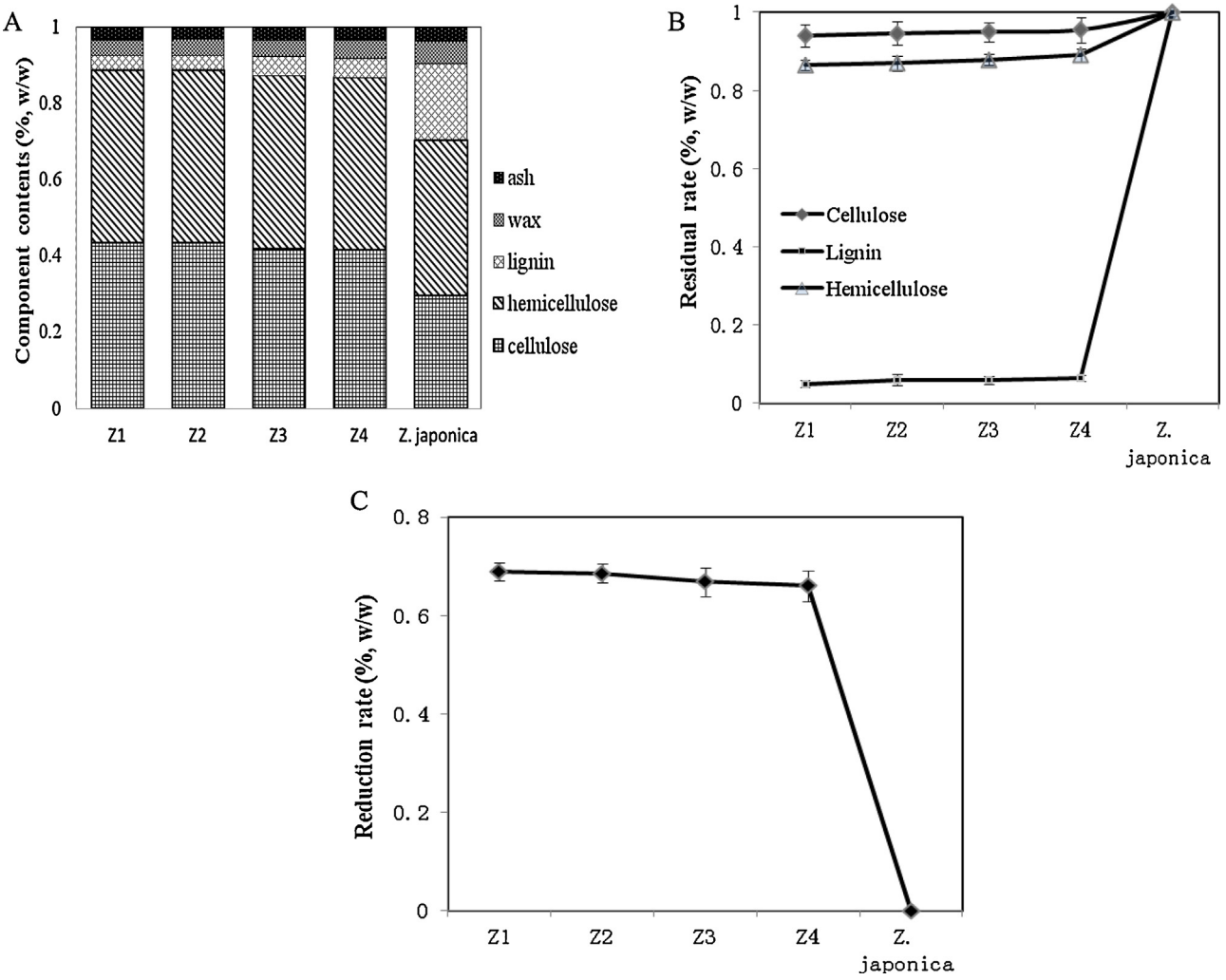

Fig. 4. The component contents of *Zoysia japonica*, Z_1, Z_2, Z_3 and Z_4 samples (A), lignocellulose residual rate after pretreatment (B), and mass loss of *Zoysia japonica* after pretreatment (C).

filtrate. The recycled AMIMCl was used to extract cellulose, as described in Sections 2.4 and 2.5.

2.7. Characterization

2.7.1. XRD

The crystal structure of alumina-doped MgO was studied using an XRD analyzer (Rigaku D/max-III X-ray diffractometer) set at 40 kV and 100 mA. Wide-angle X-ray intensities were collected for 2θ, ranging from 30° to 70°, with a step scanning rate of 8°/min and step increment of 0.04°. The crystal structures of microcrystalline cellulose (MCC), regenerated cellulose from MCC (Cel_{MCC}) and Z_1 samples (Cel_{Z1}) were studied using an XRD analyzer (Rigaku D/max-III X-ray diffractometer) set at 40 kV and 30 mA. Wide-angle X-ray intensities were collected for 2θ, ranging from 3° to 60°, with a step scanning rate of 8°/min and step increment of 0.04°.

2.7.2. FTIR

All samples were ground into a powder and vacuum-dried for 24 h. The IR spectra of the samples were recorded using an FTS6000 Fourier Transform IR spectrometer (Bio-rad, USA). Test specimens were prepared according to the KBr disk method.

2.7.3. NMR

Solid-state cross-polarization/magic angle spinning ^{13}C NMR spectra of the microcrystalline cellulose and regenerated cellulose were obtained using a Bruker Infinityplus-400 NMR spectrometer. The instrument was equipped with a 4 mm MAS probe and was operated at a frequency of 100.37 MHz. The structure of AMIMCl

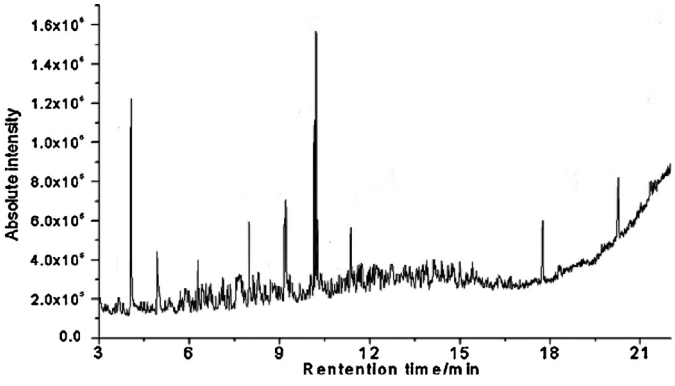

Fig. 5. GC–MS chromatograms of degraded *Z. japonica* (DZ).

in D_2O at room temperature was determined by ^1H NMR spectroscopy. Analysis was carried out on a Mercury Vx-300 with a 5 mm BBO probe at a frequency of 100.61 MHz.

2.7.4. TGA

The thermal stability of AMIMCl was investigated using a TG209 TGA instrument (NETZSCH, Ltd., Germany). Weight loss was recorded in the range of 0 to 550 °C, and the sample was heated at a rate of 10 °C/min.

2.7.5. SEM

The original *Z. japonica* and pretreated samples, obtained by air drying method, were fixed to a metal-base specimen holder using double-sided sticky tape. The samples were then coated with gold using a vacuum sputter-coater. Afterwards, the fracture surfaces were observed using an S-3700 N scanning electron microscope (Hitachi, Ltd., Japan).

2.7.6. GC–MS

DZ sample was detected using a GC–MS (Shimazu QP2010S) with an SHRXI-5 MS column. The column temperature program was set 50–280 °C (10 °C/min, hold for 20 min).

2.7.7. Crystallinity measurement

The crystallinity index, defined by the infrared ratio $A_{1428\,cm} - 1/A_{898\,cm} - 1$ (Fu & Mazza, 2011), was measured using a Nicolet-380 FT-IR spectrometer.

3. Results and discussion

3.1. Characteristics of alumina-doped MgO

Fig. 1 shows the similar XRD curves of alumina-doped MgO and the solid alkali used for the fourth time. The distinct diffracted intensities of Al_2O_3 were observed at 2θ value of 37.4°, 46.8°, and 67.3°. The more distinct diffracted intensities were observed from MgO, where the diffraction angles of 42.9° and 62.3° appeared.

3.2. Characteristics of AMIMCl

The process developed in the current study (Wu et al., 2004; Zhang, Wu, Zhang, & He, 2005) was successfully used to synthesize AMIMCl. The FTIR spectrum of AMIMCl (Fig. 2A) shows the peaks at the following wavenumbers (in cm^{-1}): 3058 (C=C–H stretching vibration), 1644 (C=C stretching vibration in allyl), 1573 (C=N stretching vibration in imidazole ring), 1424 (–CH_2/C–H bending vibration in side chain), 1335 (C–N stretching vibration), 1175 (C–H bending vibration in imidazole ring), and 997 (C–H rocking vibration in allyl). The peak at 3382 cm^{-1} corresponds to trace water accumulated due to the hygroscopicity of AMIMCl. The FTIR spectrum of the regenerated AMIMCl is similar to the spectrum of the as-synthesized AMIMCl, and shows the same peaks.

The ^1H NMR spectrum of AMIMCl (Fig. 2B) shows the peaks corresponding to the following chemical shifts (in ppm): $\delta = 4.85$, $\delta = 5.56$, $\delta = 6.05$, $\delta = 3.93$, and $\delta = 8.87$. These shifts are related to hydrogen atoms 1, 2, 3, 4, and 7, respectively. The peak at $\delta = 7.53$ is related to hydrogen atoms 5 and 6. The peaks in the ^1H NMR spectrum of the regenerated AMIMCl are similar to those in this spectrum except for the peak at $\delta = 3.41$, which corresponds to the signal for trace water.

The TGA curve for AMIMCl is shown in Fig. 2C. In the thermal degradation process, the ionic liquid was stable below 200 °C. The weight loss (nearly 20%) below 200 °C was caused by the evaporation of water and traces of remaining reactant. The decomposition temperature corresponding to the maximum rate of weight loss (T_d) was 285.1 °C, and the corresponding weight loss between 200 °C and 300 °C was nearly 80%. During the rapid decomposition process, the chloride anion decomposed through dealkylation, whereas the cation simultaneously underwent alkyl migration and elimination (Liu et al., 2012).

3.3. Pretreatment effect on Z. japonica

The structures of *Z. japonica* treated with alumina-doped MgO were observed using an S-3700N scanning electron microscope (Hitachi, Ltd., Japan). Fig. 3 shows that the structures of *Z. japonica* were destroyed by pretreatment and the surfaces of the material became rougher after pretreatment. The pretreatment created greater pore volume in the small pore region in comparison with that of the untreated sample. Pretreatment of *Z. japonica* loosened the lignocellulosic matrix, weakened intermolecular forces, and destroyed intramolecular and intermolecular hydrogen bonds, causing a more open three-dimensional organization of the cellulose, lignin, and hemicellulose polymers (Clements, 2003).

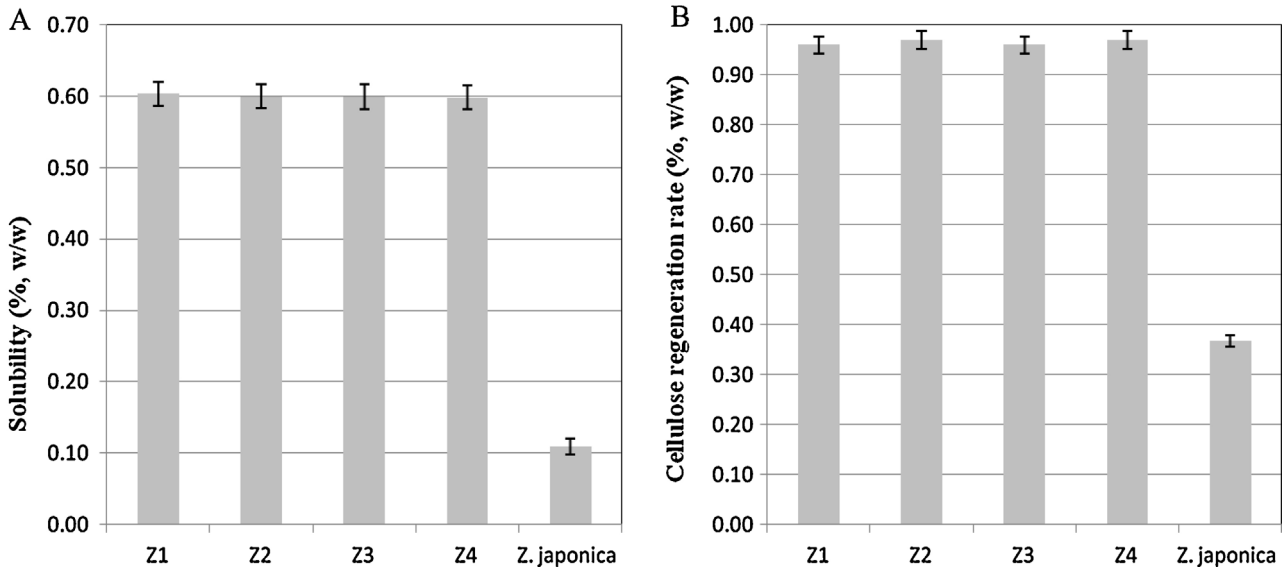

Fig. 6. *Zoysia japonica*, Z_1, Z_2, Z_3 and Z_4 samples dissolution in AMIMCl (A), and cellulose regeneration (B).

Table 1
GC–MS detectable compounds in the pretreated samples with alumina-doped MgO.

Compound name	Retention time (min)	Relative composition by area (%)[a]
2(3H)-Dihydro-4,5-dimethyl-furanone	4.501	1.82
1-Octanol	5.125	3.19
2,6-Dimethyl-phenol	6.378	2.37
2-Ethyl-6-methylphenol	7.868	2.16
2-Ethyl-5-propyl-Phenol	9.185	5.25
1-Isopropyl-2-methoxy-4-methylbenzene	10.153	3.58
2,6-Bis(1-methylethyl)-phenol	11.225	5.33
1,3,5-Tris(1-methylethyl)-benzene	17.808	1.69
Dehydroabietic acid	20.353	1.87

[a] Total area was obtained based on the integration of 26 major peaks, without including the small peaks with an area % <1.5%.

A comparison of the lignocellulosic content of Z_1, Z_2, Z_3 and Z_4 samples is shown in Fig. 4A. The cellulose and hemicellulose contents of *Z. japonica* treated with alumina-doped MgO increased relative to that of the original *Z. japonica* samples. However, the lignin content decreased. There was almost no change among the lignocellulosic content of Z_1, Z_2, Z_3 and Z_4 samples. Lignin provides a robust linkage between polysaccharide chains that hinders chemical accessibility to cellulose (Zhang & Lynd, 2004). As mentioned above, pretreatment significantly reduced the lignin content. Furthermore, levels of wax and ash were somewhat reduced. Fig. 4B and C shows the lignocellulose residual rate and mass loss of *Z. japonica* after pretreatment, respectively. Pretreatment reduced the mass of the *Z. japonica* sample significantly. However, lignin accounted for most of the mass loss, and the cellulose and hemicellulose mass were not substantially reduced. Chemical bonds between lignin and hemicelluloses form lignin–carbohydrate complexes in plant cell walls. The main bonds include ester and ether linkages (Sun, Fang, & Goodwin, 1999; Sun, Lawther, & Banks, 1996). These results, combined with the analysis of the scanning electron microscopy results, demonstrate that pretreatment with alumina-doped MgO effectively disrupted the lignocellulose structure of *Z. japonica*.

The GC–MS spectrum of DZ sample is displayed in Fig. 5. The possible degradation mechanisms for *Z. japonica* in water-ethanol co-solvents may be attributed to hydrolysis occurred at ether bonds in lignin. In lignin structure, ether bonds are the major connections among the three types of phenyl propanol monomers (Adler, 1977). Under the effect of alumina-doped MgO, hydrolysis occurred at ether bonds to form monomeric phenolic, alcohols and furanone. In DZ sample, as shown in Table 1, the major identified compounds are almost exclusively monomeric phenolic and derivatives compounds with alkyl substituents mainly -methyl, -ethyl, and a few propyl and butyl groups. Typical compounds are 2-ethyl-5-propyl-phenol, diethyl-phenol, 2-ethyl-6-methylphenol, 2,6-bis (1-methylethyl)-phenol, and 1-isopropyl-2-methoxy-4-methylbenzen, which can be ascribed to the cleavage of C_α/C_β, or C_β/C_γ, or reductive cleavage of α-*O*-4 and β-*O*-4 linkages of lignin at a high temperature (Cantrell et al., 2005; Sun et al., 2010). The alcohols and furanone, such as 1-octanol, and dihydro-4, 5-dimethyl-(3H)-furanone, could be generated by both of the cleavage of ether linkages and the lignin side chains (Leclercq et al., 2001; Xie et al., 2006).

3.4. Dissolution of cellulose in AMIMCl

AMIMCl was used to dissolve the cellulose in *Z. japonica*, Z_1, Z_2, Z_3 and Z_4 samples. Fig. 6A shows the solubility of these samples in AMIMCl. *Z. japonica* treated with alumina-doped MgO presented obvious solubility in AMIMCl. The similar high solubility of Z_1, Z_2, Z_3 and Z_4 samples showed that alumina-doped MgO had strong stability, which can be recycled and used repeatedly. Ultrasonication improved the solubility because it facilitated the penetration and diffusion of AMIMCl in the entire structure of the samples (Liu et al., 2013). The lower solubility of *Z. japonica* confirms the enhancement of cellulose solubilization by pretreatment. The cellulose regeneration rate (Fig. 6B) of Z_1, Z_2, Z_3 and Z_4 samples maintained higher levels compared with *Z. japonica*.

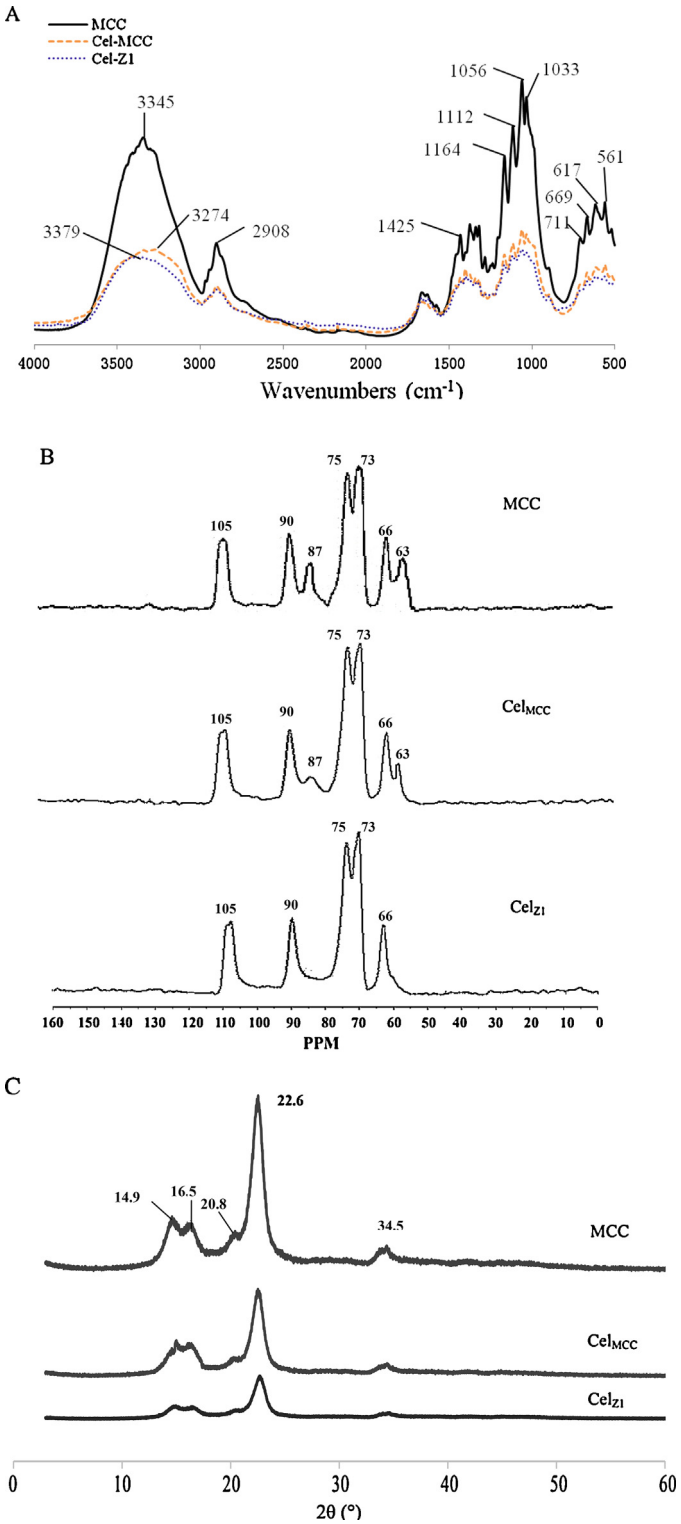

Fig. 7. FTIR spectra (A), ^{13}C NMR spectra (B), and XRD patterns (C) of microcrystalline cellulose (MCC) and regenerated cellulose from MCC (Cel_{MCC}) and Z_1 samples (Cel_{Z1}).

3.5. Characterization of regenerated cellulose

To demonstrate that no other components were mixed with the regenerated cellulose, we used FTIR and ^{13}C NMR to compare microcrystalline cellulose (column chromatography grade; 99.99% purity) with regenerated cellulose from MCC (Cel_{MCC}) and Z_1 samples (Cel_{Z1}). As shown in Fig. 7A, the FTIR spectra of both regenerated cellulose are comparable to that of microcrystalline cellulose. The spectra show similar absorbance peaks (positions listed in cm^{-1}): 3379–3274 (—O—H stretching vibration), 2908 (C—H stretching vibration), 1425 (—CH_2 stretching vibration), 1164 (C—O—C—O—C stretching vibration), 1112 (secondary alcohol C—O stretching vibration), 1056 (primary alcohol C—O stretching vibration), and 711–669 (O—H plane bending vibration). FTIR spectra indicate no obvious changes in the chemical groups of microcrystalline cellulose and Cel_{MCC}. New absorption peaks do not appear in the FTIR spectra after the pretreatment with alumina-doped MgO. But the intensity of most peaks decreased after pretreatment with solid alkali, showing that the crystallinity decreased (Wang, Li, Cao, & Tang, 2011).

Fig. 7B shows the ^{13}C NMR spectra of microcrystalline cellulose (MCC) and regenerated cellulose from MCC (Cel_{MCC}) and Z_1 samples (Cel_{Z1}). The spectra of microcrystalline cellulose and Cel_{MCC} almost have the same characteristic peaks at 105 (C1), 90 (C4, crystalline), 87 (C4, amorphous), 75 (C3/C5), 73 (C2), 66 (C6, crystalline), and 63 (C6, amorphous) ppm. But the peaks of Cel_{MCC} were weakened at 87 ppm and 63 ppm, which can be regarded as evidence that crystallinity decreased. The spectrum of Cel_{Z1} also has characteristic peaks at 105, 90, 75, 73, and 66 ppm, but peaks at 87 and 63 ppm are not present. The reduced intensities of all the characteristic peaks of regenerated cellulose suggest that the crystallinity of the regenerated cellulose was lower.

The average crystallinity value of regenerated cellulose from pretreated Zoysia japonica, determined to be 1.055, was lower than the reported general value of 1.469 (Fu & Mazza, 2011). Fig. 7C shows the XRD curves of the MCC, Cel_{MCC} and Cel_{Z1} samples. The diffracted intensity of Cel_{MCC} sample at 2θ values was less intense than the distinct diffracted intensity of MCC sample. The more distinct decrease in diffracted intensity was observed from Cel_{Z1} sample, where the diffraction angles of 14.9°, 16.5°, 20.8°, and 34.5° nearly disappeared. It is resulted from the crystalline form destruction during the dissolution process in AMIMCl (Li et al., 2013).

4. Conclusions

Pretreatment with alumina-doped MgO disrupted the lignocellulose structure and significantly reduced the lignin content of the *Z. japonica*. Under the effect of alumina-doped MgO, hydrolysis occurred at ether bonds to form monomeric phenolic, alcohols and furanone. After pretreatment, *Z. japonica* showed significant solubility in AMIMCl. The similar high solubility of Z_1, Z_2, Z_3 and Z_4 also proved that alumina-doped MgO had strong stability, which can be recycled and used repeatedly. The regenerated cellulose was similar to microcrystalline cellulose according to FTIR and NMR analyses. Compared to microcrystalline cellulose, only the crystallinity of the regenerated cellulose decreased.

Acknowledgment

We are grateful for financial support by the “Double Five” Science and Technology Project of the Colleges and Universities in Tianjin, China (SW20080004).

References

Adler, E. (1977). Lignin chemistry: Past, present and future. *Wood Science and technology*, *11*, 169–218.

Benoit, G., Peter, H., & Moreau, J. E. (2004). Supported ionic liquids: ordered mesoporous silicas containing covalently linked ionic species. *Chemical Communications*, *15*, 1768–1769.

Cantrell, D. G., Gillie, L. J., Lee, A. F., & Wilson, K. (2005). Structure–reactivity correlations in MgAl hydrotalcite catalysts for biodiesel synthesis. *Applied Catalysis A*, *287*(2), 183–190.

Clements, J. H. (2003). Reactive applications of cyclic alkylene carbonates. *Industrial & Engineering Chemistry Research*, *42*(4), 663–674.

Deng, Y. C. (2003). Ionic liquids – The green material in the 21st century. *Chinese University Technology Transfer*, *10*, 33–35.

Ebiura, T., Echizen, T., Ishikawa, A., Murai, K., & Baba, T. (2005). Selective transesterification of triolein with methanol to methyl oleate and glycerol using alumina loaded with alkali metal salt as a solid-base catalyst. *Applied Catalysis A*, *283*(1–2), 111–116.

Fu, D. B., & Mazza, G. (2011). Aqueous ionic liquid pretreatment of straw. *Bioresource Technology*, *102*, 7008–7011.

Heinze, T., & Liebert, T. (2001). Unconventional methods in cellulose functionalization. *Progress in Polymer Science*, *26*, 1689–1762.

Klemm, D., Philipp, B., Heinze, T., Heinze, U., & Wagenknecht, W. (1998). *Comprehensive cellulose chemistry*. Weinheim: Wiley-VCH.

Leclercq, E., Finiels, A., & Moreau, C. (2001). Transesterification of rapeseed oil in the presence of basic zeolites and related solid catalysts. *Journal of the American Oil Chemical Society*, *78*(11), 1161–1165.

Li, C., Knierim, B., Manisseri, C., Arora, R., Scheller, H. V., Auer, M., et al. (2010). Comparison of dilute acid and ionic liquid pretreatment of switchgrass: Biomass recalcitrance, delignification and enzymatic saccharification. *Bioresource Technology*, *101*, 4900–4906.

Li, W. Z., Ju, M. T., Wang, Y. N., Liu, L., & Jiang, Y. (2013). Separation and recovery of cellulose from Zoysia japonica by 1-allyl-3-methylimidazolium chloride. *Carbohydrate Polymers*, *92*, 228–235.

Liu, D. T., Xia, K. F., Cai, W. H., Yang, R. D., Wang, L. Q., & Wang, B. (2012). Investigations about dissolution of cellulose in the 1-allyl-3-alkylimidazolium chloride ionic liquids. *Carbohydrate Polymers*, *87*, 1058–1064.

Liu, L., Ju, M. T., Li, W. Z., & Hou, Q. D. (2013). Dissolution of cellulose from AFEX-pretreated Zoysia japonica in AMIMCl with ultrasonic vibration. *Carbohydrate Polymers*, *98*, 412–420.

Oh, S. Y., Yoo, D. I., Shin, Y., Kim, H. C., Kim, H. Y., & Chung, Y. S. (2005). Crystalline structure analysis of cellulose treated with sodium hydroxide and carbon dioxide by means of X-ray diffraction and FTIR spectroscopy. *Carbohydrate Research*, *340*(15), 2376–2391.

Pang, C. H., Xie, T. J., Lin, L., Zhuang, J. P., Liu, Y., Shi, J. B., et al. (2012). Changes of the surface structure of corn stalk in the cooking process with active oxygen and MgO-based solid alkali as a pretreatment of its biomass conversion. *Bioresource Technology*, *103*, 432–439.

Peterson, G. R., & Scarrah, W. P. (1984). Rapesseed oil transesterification by heterogeneous catalysis. *Journal of the American Oil Chemical Society*, *61*(10), 1593–1597.

Ren, Q., Wu, J., Zhang, J., He, J. S., & Guo, M. L. (2003). Synthesis of 1-allyl, 3-methylimidazolium-based room temperature ionic liquid and preliminary study of its dissolving cellulose. *Acta Polymerica Sinica*, *3*, 448–451.

Sun, G. L. (2012). *Catalytic hydrogenation degradation of lignin* (Doctor thesis). Beijing University of Chemical Technology.

Sun, H., Ding, Y. Q., Duan, J. Z., Chen, P., Lou, H., & Zheng, X. M. (2010). Transesterification of sunflower oil to biodiesel on ZrO_2 supported La_2O_3 catalyst. *Bioresource Technology*, *101*, 953–958.

Sun, R. C., Fang, J. M., & Goodwin, A. (1999). Fractionation and characterization of ball-milled and enzyme lignins from abaca fibre. *Journal of the Science of Food and Agriculture*, *79*(8), 1091–1098.

Sun, R. C., Lawther, J. M., & Banks, W. B. (1996). Effects of extraction time and different alkalis on the composition of alkali-soluble wheat straw lignins. *Journal of Agricultural and Food Chemistry*, *44*(12), 3965–3970.

Swatloski, R. P., Spear, S. K., Holbrey, J. D., & Rogers, R. D. (2002). Dissolution of cellulose with ionic liquids. *Journal of the American Chemical Society*, *124*(18), 4974–4975.

Wang, X. J., Li, H. Q., Cao, Y., & Tang, Q. (2011). Cellulose extraction from wood chip in an ionic liquid 1-allyl-3-methylimidazolium chloride (AmimCl). *Bioresource Technology*, *102*, 7959–7965.

Wang, Y. (2012). *Study on degradation of lignin catalyzed by solid base catalysts and the synthesis and modification of polyurethane* (Doctor thesis). Beijing University of Chemical Technology.

Wu, J., Zhang, J., Zhang, H., He, J. S., Ren, Q., & Guo, M. L. (2004). Homogeneous acetylation of cellulose in a new ionic liquid. *Biomacromolecules*, *5*(2), 266–268.

Xie, W. L., Peng, H., & Chen, L. G. (2006). Calcined Mg–Al hydrotalcites as solid base catalysts for methanolysis of soybean oil. *Journal of Molecular Catalysis A: Chemica*, *246*(1–2), 24–32.

Zhang, H., Wu, J., Zhang, J., & He, J. S. (2005). 1-Allyl-3-methylimidazolium chloride room temperature ionic liquid: A new and powerful nonderivatizing solvent for cellulose. *Macromolecules*, *38*(20), 8272–8277.

Zhang, J. M., Lv, Y. X., & Luo, N. (2011). Application research progress of ionic liquids in cellulose chemistry. *Polymer Bulletin*, *10*, 138–153.

Zhang, Y. H. P., & Lynd, L. R. (2004). Toward an aggregated understanding of enzymatic hydrolysis of cellulose: Noncomplexed cellulase systems. *Biotechnology and Bioengineering*. *88*, 797–824.

Zhu, S. D., Wu, Y. X., Chen, Q. M., Yu, Z. N., Wang, C. W., Jin, S. W., et al. (2006). Dissolution of cellulose with ionic liquids and its application: A minireview. *Green Chemistry*, *8*, 325–327.